Power Control for AP-Based Wireless Networks under the SINR Interference Model: Complexity and Efficient Algorithm Development

Shuang Li, Eylem Ekici, and Ness Shroff

Abstract—In this paper, the power control problem is considered for access-point based wireless networks under the SINR interference model. This problem is NP hard in terms of the number of APs in the network, and if not designed properly can have high polynomial complexity in terms of the power levels. We first separate the overall problem into two sub-problems using the primal-dual method. We then develop an efficient algorithm under the SINR-interference model that uses only two power levels to solve a subproblem of the overall power control problem, which we call the utility-independent power control (UIPC) subproblem. This approach allows the optimality gap of the UIPC subproblem to be bounded. Moreover, a two-stage iterative algorithm is developed that solves the overall power control problem within a small neighborhood of the global optimum. This offline algorithm has a significantly lower computational complexity than the globally optimal algorithm. Further, based on the structure of the iterative algorithm, an efficient heuristic two-stage greedy algorithm is proposed with low polynomial time complexity. Finally, numerical results are provided to demonstrate the efficacy of our solution.

Index Terms—Power control, SINR, Wireless Networks, Complexity

I. Introduction

Access point (AP)-based wireless networks, such as wireless local area networks (WLANs), have increasingly become the primary means of network connectivity for indoor and hotspot environments. With dense deployment of access points, sub-networks sharing the ISM band contend for channel access, resulting in inefficient exploitation of limited wireless resources. Since the demand for wireless access to a backbone network is expected to increase, more effective use of the available capacity is necessary to sustain desired performance levels.

The utility maximization problem for wireless systems has been extensively investigated in the past ([7], [8], [12], [13]). The scheduling problem, which is NP-hard in number of nodes in a wireless network, has been solved using low complexity distributed algorithms, which achieve a provable fraction of the optimal ([2], [3], [9], [15]). However, these solutions do not apply to cases where the *link capacity is a function of SINR*, and *power control* is considered, which is precisely the focus

S. Li is with the Department of Computer Science and Engineering, Ohio State University, Columbus, OH, 43210.
E-mail: li.908@osu.edu

E. Ekici is with the Department of Electrical and Computer Engineering, Ohio State University, Columbus, OH, 43210.
E-mail: ekici@ece.osu.edu

N. Shroff is with the Department of ECE and CSE, Ohio State University, Columbus, OH, 43210.
E-mail: shroff@ece.osu.edu

of this paper. Traditionally, its solution is obtained through a brute-force search of exponential complexity. We show that it is indeed exponentially complex in the number of APs and has high polynomial complexity in terms of power levels even for small problem instances involving two access points and two users. We then propose lower complexity solutions that yield results within a small neighborhood of the optimum, and develop polynomial-time heuristics.

The power control problem has been investigated in the literature under different constraints. Based on a high SINR model, the problem has been converted to a geometric programming problem in [4] and solved without considering scheduling. In [6], power allocation for two transmitters has been solved analytically using continuous relaxation. However, efficient optimal solutions for M transmitters is not developed due to the non-convexity of the capacity region. Therefore, only an iterative water-filling scheme is proposed in [6], and its performance is demonstrated through simulations. When discrete power levels are considered [1], the brute-force search solution is of $O(N^M)$, where N is the number of power levels, and M is the number of transmitters. The uplink power allocation problem has also been investigated in [10] with the assumption that channel gains between all transmitter-receiver pairs and the noise levels are the same. As such, the problem formulation in [10] constitutes only a limited subset of the general problem we are tackling in this paper.

To solve the power control problem efficiently, we propose a new algorithm that is based on obtaining a suboptimal solution to a subproblem of the overall power control problem, which we call the utility-independent power control (UIPC) subproblem in the dual space for arbitrary SINR values, with a significantly reduced complexity. This suboptimal solution is utilized in every iteration of the subgradient method to solve the overall power control problem. Our proposed two-stage iterative algorithm is shown to converge to a small neighborhood of the global optimal solution. Scheduling decisions follow as a byproduct of our algorithm. The algorithm is of $O(1)$ complexity for some easily identified subset of problems involving two transmitters ($M = 2$), and $O(N+T)$ for others, where T is the number of iterative steps. For larger M, the complexity is reduced from $O(N^M)$ to $O(N^{M/2})$. Based on the structure of our proposed iterative algorithm, *a two-stage greedy heuristic* with polynomial time complexity is developed for an arbitrary number of transmitters M. The contributions of this paper can be summarized as follows:

- We propose an asymptotically optimal algorithm that significantly reduces the complexity of solving the power control problem for one-hop AP-based wireless networks under the SINR interference model.
- A polynomial-time greedy algorithm is proposed inspired by the structure of the aforementioned asymptotically optimal algorithm.

The remainder of the paper is organized as follows: We describe the system model in Section II. In Section III, we present our approximate solution to the UIPC subproblem and bound the optimality gap. Then we solve the overall power control problem with an efficient two-stage iterative algorithm that is asymptotically optimal. A polynomial time greedy algorithm is also presented. Numerical evaluation results are discussed in Section IV. We conclude the paper in Section V. Throughout the paper, proofs of lemmas and propositions are presented in our online technical report [11].

II. THE SYSTEM MODEL

We consider a wireless network with M access points. We focus on a generic time instance where each AP establishes a single-hop downlink to a given user, where each link is indexed from 1 to M. Let L be the set of all links. $\vec{P}$ denotes the global power assignment for the access points. Let the set of feasible power assignments be denoted by Π, such that the power P_i allocated on each link i is non-negative and bounded by a maximum value P_{max}, i.e., $0 \leq P_i \leq P_{max}$. Let g_{ij} be the channel gain from the transmitter of link j to the receiver of link i. The normalized channel gain is defined as $f_{ij} = g_{ij}/g_{ii}$. Let N_i be the noise at the receiver of link i. Then $\tau_i = N_i/g_{ii}$ is defined as the normalized noise at the receiver of link i. Let $\vec{r} = [r_i, \ i = 1, \cdots, M]$ denote the vector of data rates. $r_i = u(\vec{P}) = \log(1 + \frac{g_{ii}P_i}{\sum_{j \neq i} g_{ij}P_j + N_i}) = \log(1 + \frac{P_i}{\sum_{j \neq i} f_{ij}P_j + \tau_i})$, where $u(\cdot)$ is the rate-power function. For a given $SINR$, each link adopts an appropriate modulation and coding scheme to achieve its maximal rate. Let $\vec{r}$ represent the link allocation vector. Given power constraints and channel realizations, $R = \{u(\vec{P}), \vec{P} \in \Pi\}$ is the set of all feasible link rate allocations. We use R and "Capacity Region" interchangeably in this paper. Note that R need not be convex. Let $Co(R)$ be the *convex hull* of R, which is closed and bounded.

Let $\vec{a} = [a_i, \ i = 1, \cdots, M]$ be the actual rates injected into the network by the transmitters. Each user (receiver) is associated with a utility function $U_i(a_i)$, which reflects the satisfaction of the user i when receiving data at rate a_i. We assume that the utility function $U_i(\cdot)$ is strictly concave, non-decreasing, and twice continuously differentiable. We take log form in this paper to guarantee proportional fairness. The primal problem is defined as follows:

$$\max \sum_{i=1}^{M} U_i(a_i)$$

$$\text{subject to } r_i - a_i \geq 0, \ \forall i = 1, 2, \cdots, M$$
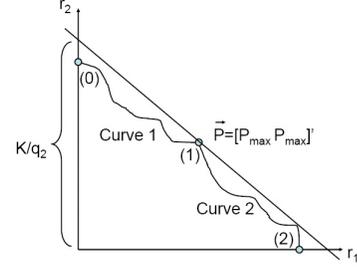
$$\vec{r} \in Co(R) \quad (1)$$

Fig. 1. Capacity region of two transmitter-receiver pairs. Boundary points with $r_1 = 0$ and $r_2 = 0$ are called (0) and (2), respectively. The point where both transmitters are using the maximum power is called (1).

III. SOLUTION AND ALGORITHM DESIGN

The dual objective function of (1) is of the following form:

$$D(\vec{q}) = \max_{\vec{r} \in R} \left(\sum_{i=1}^{M} U_i(a_i) + \sum_{i=1}^{M} q_i(r_i - a_i) \right) \quad (2)$$

Given $\vec{q}$, Equation (2) is decomposed to subproblem 1:

$$\sum_{i=1}^{M} \max_{a_i} (U_i(a_i) - q_i a_i) \quad (3)$$

and subproblem 2, called *utility-independent power control* (UIPC):

$$\max_{\vec{r} = u(\vec{P}), \vec{P} \in \Pi} \sum_{i=1}^{M} q_i r_i. \quad (4)$$

Remark: (3) is composed of separable convex problems, the solution to which is $a_i^* = U_i'^{-1}(q_i)$. The solution to Equation (4) is still nontrivial. Note that when r_i is restricted to be either 0 or a predetermined fixed constant, a special version of (4) reduces to the classical Maximum Independent Set problem [5] although the proof needs some modification [11].

We first focus on the solution to UIPC subproblem in the two-transmitter case and bound the optimality gap in Section III-A. Then we generalize the solution to the overall power control problem (1) in M-transmitter cases ($M \geq 2$) in Section III-B. Inspired by the asymptotically optimal solution, we develop a polynomial-time greedy algorithm in Section III-C.

A. Two-Transmitter Case

A system with only two APs (two transmitter-receiver pairs) is a special case where we can categorize the capacity region with $\vec{r} = [r_1 \ r_2]'$ in a plane. In this case, the boundary of the capacity region is composed of two curves, referred to as Curve 1 and Curve 2, which reflect the relationship between r_2 and r_1 with $P_2 = P_{max}$ and $P_1 = P_{max}$, respectively. Let $K = q_1 r_1 + q_2 r_2$, which is the objective function of (4) with two transmitter-receiver pairs. Then, $r_2 = -\frac{q_1}{q_2} r_1 + \frac{K}{q_2}$ is a line, with the tangent point to the capacity region corresponding to the optimal values of $\vec{P}$. For Curve 1, $r_1 = \log(1 + \frac{P_1}{P_{max}f_{12} + \tau_1})$, and $r_2 = \log(1 + \frac{P_{max}}{P_1 f_{21} + \tau_2})$. Thus, the function of r_2 in r_1 can be written as:

$$r_2 = \log(1 + \frac{P_{max}}{Ae^{r_1} + (\tau_2 - A)}) \quad (5)$$

where $A = f_{21}(P_{max}f_{12}+\tau_1) > 0$. Curve 2 has similar forms. $P_1 = P_{max}$ on Curve 1 and $P_2 = P_{max}$ on Curve 2.

Let K^* be the optimal solution to (4), and K_0, K_1, and K_2 be the values of the objective function of (4) at points (0), (1) and (2) (called extreme points), respectively, as shown in Figure 1. We define the gap as $\Delta = K^* - \max(K_0, K_1, K_2)$ and the ratio-wise gap as $\frac{\Delta}{P_{max}}$. The shapes of the capacity region are characterized by the proposition below:

Proposition 3.1: Both Curve 1 and Curve 2 fall into one of only three categories: convex, concave and partly-convex-partly-concave depending on different noise and interference levels.

Proof: See [11]. ■

We interpret how the shape of the curve shape changes from concave, to partly concave and partly convex, to convex, and the physical meaning of the conditions we have discussed so far. Equation (5) may be rewritten as:

$$r_2 = \log(1 + \frac{P_{max}}{A(e^{r_1} - 1) + \tau_2}) \qquad (6)$$

where $e^{r_1} - 1$ is $SINR_1$, A is the interference at receiver 2 when $SINR_1 = 1$. Therefore, $A(e^{r_1} - 1)$ is the scaled interference. When τ_2 is large, which corresponds to the sufficient and necessary condition for concavity, noise dominates, leading to a concave shape. When τ_2 is small enough, which corresponds to the sufficient and necessary condition for convexity, interference dominates so that the curve is concave. When τ_2 falls in between, it dominates r_1 partly, which causes a concave shape, and it is dominated by r_1 partly, which results in a convex shape. Another observation is that the capacity region shrinks with τ_2 increasing. The sufficient condition $\tau_2 \le A$ for convexity is interpreted as noise less than scaled interference at receiver 2. An example of this could be $\tau_2 \le \frac{1}{k}$ of the interference at receiver 2 when $SINR_1 = k$. The denominator of $\frac{P_{max}}{A(e^{r_1}-1)+\tau_2}$ in Equation (6) is composed of Ae^{r_1} and a non-positive constant term, which leads to convexity when the sufficient condition is satisfied.

Based on the capacity region characterization, we summarize the sub-optimality of UIPC subproblem in the proposition below.

Proposition 3.2: If $P_{max} \ge \max(\frac{\tau_1}{f_{12}f_{21}} - \frac{\tau_2}{f_{21}}, \frac{\tau_2}{f_{12}f_{21}} - \frac{\tau_1}{f_{12}})$ (both curves are convex), $K^* = \max(K_0, K_1, K_2)$; else, Δ, the gap between the optimal solution to (4) and the solution by taking extreme values at points 0, 1 and 2, are upper bounded by $\max(q_1 \log(1 + \frac{P_{max}}{P_{max}f_{12}+\tau_1}), q_2 \log(1 + \frac{P_{max}}{P_{max}f_{21}+\tau_2}))$; The upper bound of $\frac{\Delta}{P_{max}}$, the ratio-wise gap, is $\max(\frac{q_1}{\tau_1^2}, \frac{q_2}{\tau_2^2})$.

Proof: See [11]. ■

Note that a large τ_1 is undesirable both from the point of view of resulting in a smaller capacity region and resulting in a large Δ. However, even though Δ is large, the ratio-wise upper bound diminishes with increasing τ_1.

B. General M-transmitter ($M \ge 2$) cases

Intuitively we are no longer able to split the capacity boundary into two parts and further categorize each part separately as in two-transmitter cases. By introducing a new concept, *equi-power line projection*, we are able to analyze the mapping of the capacity region onto each $r_i - r_j$ plane.

Given $\vec{\breve{P}} = (P_3, \cdots, P_M)$, the *equi-power line projection* is composed of two curves: $r_2 = \log(1 + \frac{P_{max}}{(e^{r_1}-1)(P_{max}f_{12}+\vec{F_1}'\vec{\breve{P}}+\tau_1)f_{21}+\vec{F_2}'\vec{\breve{P}}+\tau_2})$ and $r_1 = \log(1 + \frac{P_{max}}{(e^{r_2}-1)(P_{max}f_{21}+\vec{F_2}'\vec{\breve{P}}+\tau_2)f_{12}+\vec{F_1}'\vec{\breve{P}}+\tau_1})$ on r_1-r_2 plane where $\vec{F_1} = (f_{13}, \cdots, f_{1M})$ and $\vec{F_2} = (f_{23}, \cdots, f_{2M})$. Proposition 3.1 is still true for each *equi-power line projection*. Proposition 3.2 no longer holds because of the higher dimensional capacity region.

Now we are more interested in how the suboptimality of the solution to UIPC subproblem (Equation (4)) affects the dual problem $\min D(\vec{q})$ of Equation (2).

$$\min \hat{D}(\vec{q})$$
$$\vec{r} \in \hat{R} \qquad (7)$$

Define $\hat{R} = \{$Points 0, 1, 2$\}$. The new dual problem is (7) where $\hat{D}$ is the same as D except for the domain of $\vec{r}$. Let $\hat{\vec{q}^*}$ be the optimal solution to the new dual problem. Let $U_i(a_i)$ take a specific form of $\beta_i log(1 + a_i)$, where β_i is the weight of user i. Then, the solution to (3) given $\vec{q}$ is $a_i^* = \frac{\beta_i}{q_i} - 1$.

Strong duality holds for the primal problem (1). The following subgradient method is used to solve the dual problem $\min D(\vec{q})$:

$$q_i(t+1) = \{q_i(t) - h_t[r_i^*(\vec{q}(t)) - \frac{\beta_i}{q_i(t)} + 1]\}^+ \quad (8)$$

To solve the new dual problem (7), we can also use the subgradient method, the time complexity of which is $O(2^M \cdot T)$ where T is the number of iterations. We assume the numbers of iterations in Equations (8) and (9) are of the same order.

$$q_i(t+1) = \{q_i(t) - h_t[\arg\max_{r_i} \sum_{i=1}^{M} q_i(t)r_i - \frac{\beta_i}{q_i(t)} + 1]\}^+. \quad (9)$$

By Proposition 3.1, in two-transmitter cases and when $P_{max} \ge \max(\frac{\tau_2}{f_{12}f_{21}} - \frac{\tau_1}{f_{12}}, \frac{\tau_1}{f_{12}f_{21}} - \frac{\tau_2}{f_{21}})$, both Curves 1 and 2 are convex. Given the same $\vec{q}(t)$, $r^*(\vec{q}(t)) = \arg\max_{\vec{r} \in \hat{R}} \sum_{i=1}^{2} q_i(t)r_i$. Starting from the same initial point, Equations (8) and (9) must converge to the same $\vec{q}$ in the same number of steps. In multi-transmitter cases, however, convex conditions are hard to derive although they exist; thus we treat each case as non-convex and propose a **preliminary subgradient-based algorithm**:

- Step 1: Compute $\hat{\vec{q}^*}$ iteratively by Equation (9) and find $\vec{r^{(j)}} = \arg\max \sum \hat{q_i^*} r_i^{(k)}$, where k is the extreme point index, and $\vec{P^*}$ that corresponds to $\vec{r^{(j)}}$.
- Step 2: Let $\vec{q(0)} = \hat{\vec{q}^*}$. Compute the convergence result $\vec{q}$ iteratively by Equation 8 and find $r_i^*(\tilde{q_i}) = \frac{\beta_i}{\tilde{q_i}} - 1$ and $\vec{\breve{P}}$ that corresponds to $\vec{r^*}(\vec{\tilde{q}})$.

We need Lemmas 3.3-3.7 to prove Theorem 3.8. Proofs of these lemmas are given in [11].

Lemma 3.3: If $h_t < \min(\frac{4\beta_1}{r_1^{(2)}+1}, \frac{4\beta_2}{r_2^{(0)}+1})$ for both Equations (8) and (9) for a given $q_i(0) > 0$, then $q_i(t) > 0, \forall t > 0$.

In practice, if we take a constant step size h, which is less than $\min(\frac{4\beta_1}{r_1^{(2)}+1}, \frac{4\beta_2}{r_2^{(0)}+1})$. Furthermore, we may get rid of $\{\cdot\}^+$ in the sub-gradient method when the step sizes satisfy the condition in Lemma 3.3. We first investigate Equation (9). By taking appropriate step sizes, i.e., $h_k > 0$, $h_k \to 0$, and $\sum_{k=1}^{\infty} h_k = \infty$, Equation (9) converges to $\vec{q}^*$ (Theorem 2.3 in [14]).

Lemma 3.4: Subgradient of $\hat{D}(\vec{q})$ at $\vec{q}^*$ is 0, i.e.,
$\arg\max_{r_i} \sum_{i=1}^{M} \hat{q}_i^* r_i - \frac{\beta_i}{q_i^*} + 1 = 0$.

Lemma 3.5: Define $d_i^t, \forall t \geq 0, i = 1, 2$ as the subgradient at $q(\vec{t})$. So, $d_i^t = r_i^*(q(\vec{t})) - \frac{\beta_i}{q_i(t)} + 1$. $\forall \epsilon > 0, \exists \delta$, s.t. $\forall h_1 < \delta$, $d_1^0 - d_1^1 < \epsilon$ and $d_2^1 - d_2^0 < \epsilon$.

The lemma below is a direct result from Lemma 3.5.

Lemma 3.6: Fixing $h_1, h_2, \cdots, h_t, \forall \epsilon, \exists \delta$, s.t. $\forall h_{t+1} < \delta$, $d_1^t - d_1^{t+1} < \epsilon$ and $d_2^{t+1} - d_2^t < \epsilon$.

In multi-transmitter cases, we also have the following lemma:

Lemma 3.7: For all $\epsilon > 0$ that are sufficiently small, $\exists \vec{\Delta}_q$, s.t. $|r_i^*(\vec{q} + \vec{\Delta}_q) - r_i^*(\vec{q})| < \epsilon, \forall i$.

Theorem 3.8: The **preliminary subgradient-based algorithm** is asymptotically optimal.

Proof: Due to page limit, we only give the proof sketch in the following. Details can be found in [11]. Our proof can be split into three parts.

First, we prove the convergence of Step 2 when $\sum h_t = \infty$ since the convergence of Step 1 is shown in Lemma 3.4. We use h_t satisfying the condition in Lemma 3.3 to get rid of $\{\cdot\}^+$ in the subgradient method. $\|\vec{d^t}\|$ can be shown to be bounded. By Theorem 2.3 in [14], $\vec{q}$ converges to $\vec{q}^*$.

Second, we show that with a sufficiently small constant step size h, $\vec{q}$ converges to $\vec{\tilde{q}}$ s.t. $\forall \epsilon, \|\vec{q}^* - \vec{\tilde{q}}\| < \frac{h}{2}(\|\vec{d^0}\| + \epsilon)$. Taking small enough constant h, we can arrange both d_1^t and d_2^t to only fluctuate around 0 in a small neighborhood. So we have $\|\vec{d^0}\| > \|\vec{d^t}\|, \forall t$. Then, we follow a similar approach as the proof of Theorem 2.1 in [14] to show $\vec{\tilde{q}}$ can be arbitrarily close to $\vec{q}^*$.

Third, we will prove $D(\vec{\tilde{q}})$ is an asymptotically optimal solution to the primal problem (1) by showing that,

$$\forall \epsilon > 0, \ |D(\vec{q}^*) - D(\vec{\tilde{q}})| < \sum_{i=1}^{M} |r_i^*(\vec{\tilde{q}}) - r_i^*(\vec{q}^*)|$$
$$+ \frac{h}{2}(\|d^0\| + \epsilon) \sum_{i=1}^{M} (\frac{\beta_i}{\min(\tilde{q}_i, q_i^*)} + r_i^*(\vec{\tilde{q}}) + |a_i^*(\tilde{q}_i)| + \frac{\beta_i}{\tilde{q}_i})$$
$$\tag{10}$$
$\blacksquare$

Solving $r_i^*(q(\vec{t}))$ for $O(T)$ times is still hard since we need to solve high-order equations in Step 2. We replace Step 2 with Step 2' and propose Algorithm 1.

• Step 2': Fix power elements that satisfy the statement in Lemma 3.9. We have a simplified method to find them as stated in Algorithm 1. Search others from 0 through P_{max} to maximize $\sum_{i=1}^{M} U_i(r_i)$.

Algorithm 1 Proposed Algorithm Achieving Asymptotic Optimality for Multi-transmitter Case

1: Compute $\vec{\hat{q}^*}$ by Equation (9) with iterations
2: $r^{(j)} \leftarrow \arg\max \sum \hat{q}_i^* r_i^{(k)}$, find corresponding $\vec{\hat{P}^*}$
3: $\hat{S}^* \leftarrow \sum_{i=1}^{M} \hat{q}_i^* r_i$ where $\vec{r}$ is decided by $\vec{\hat{P}^*}$
4: **for all** $P_j = P_{max}$ in $\vec{\hat{P}^*}$ **do**
5:     $P_j \leftarrow P_{max} - \frac{P_{max}}{N}$ and $S \leftarrow \sum_{i=1}^{M} \hat{q}_i^* r_i$ given the current power assignment
6:     **if** $\hat{S}^* > S$ **then**
7:         $Flag_j \leftarrow 1$
8:     **end if**
9:     $P_j \leftarrow P_{max}$
10: **end for**
11: **for all** P_i **do**
12:     **if** $Flag_i = 1$ **then**
13:         $P_i^* \leftarrow P_{max}$
14:     **end if**
15: **end for**
16: **for all** P_i **do**
17:     Vary P_i with $Flag_i = 0$ from 0 through P_{max} to find $P_i^* = \arg\max \sum_{i=1}^{M} U_i(r_i)$
18: **end for**
19: **return** $\vec{P^*}$

Lemma 3.9: In the M-transmitter case, at least $\lfloor \frac{M}{2} \rfloor$ power elements in the power vector that corresponds to $r_i^*(\vec{\hat{q}^*})$ are P_{max} and their counterparts in $\arg\max \sum \hat{q}_i^* r_i^{(k)}$ are P_{max} as well.

Theorem 3.10: **Algorithm 1** is asymptotically optimal.

Both the proofs of Lemma 3.9 and Theorem 1 are in [11]. The general idea of our algorithm is to move the power vector $\vec{P^*}(\vec{\hat{q}^*})$, in an approximate sense, toward the extreme point $\vec{P^*}$ where $\vec{P^*}(\vec{q^*})$ is the solution to the overall problem with binary-value search and $\vec{P^*}(\vec{\hat{q}^*})$ is the optimal solution to (4) with $\vec{q} = \vec{\hat{q}^*}$. Since it is of high time complexity to find $\vec{P^*}(\vec{\hat{q}^*})$, we search in Step 2' of Algorithm 1 more efficiently by avoiding the zigzag search in Step 2. Overall, Step 1 determines the end point of the search and Step 2' determines the direction. The time complexity of Step 2' is $O(N^{M/2})$ by Lemma 3.9. So the overall time complexity for Algorithm 1 is $O(2^M \cdot T + N^{M/2})$. When M or N is large, $O(N^{M/2})$ dominates and is much smaller than $O(N^M)$, the complexity of a combinatorial algorithm.

Remark: For the two-transmitter case, the problem can be solved in $O(1)$ time when $P_{max} \geq \max(\frac{\tau_2}{f_{12}f_{21}} - \frac{\tau_1}{f_{12}}, \frac{\tau_1}{f_{12}f_{21}} - \frac{\tau_2}{f_{21}})$, and in $O(N + T)$ time otherwise. For multi-transmitter cases ($M > 2$), such simplifying conditions on P_{max} are not easily determined. Therefore, we need to rely on the general solution method with $O(N^{M/2})$ complexity.

C. Greedy Algorithm

Algorithm 1 is of $O(1)$ complexity for some easily identified subset of problems involving $M = 2$, and $O(N + T)$ for others. For larger M, the complexity that is reduced from $O(N^M)$ to $O(N^{M/2})$, which remains exponential in the number of transmitters. Thus, we next develop an efficient heuristic polynomial-time greedy algorithm, the structure of which is guided by Algorithm 1.

We still use the iteration structures. In Step 1" (Lines 1-35 in Algorithm 2), we group APs with similar $\vec{q}$s hierarchically and fix the powers of APs with a large value in (4) at each iteration. In Step 2" (Lines 36-40), the grouping criterion becomes geographical closeness. The intuition behind Algorithm 2 is: both Steps 1" and 2" group APs in twos because the error bound of (4) is derivable (Proposition 3.2). Also, Lemma 3.9 suggests the power adjustment of at most $\frac{M}{2}$ transmitters. For the convenience of algorithm design, we define π^ϱ as a vector of M components, which is the temporary power allocation. ϱ is the group index (See Algorithm 2). $\vec{r}(\pi)$ is the corresponding rate allocation given the power allocation π. $[a]_x$ is a vector of length x and all elements are a. Both "+" and "−" in Algorithm 2 are element-wise operators. We define a function $Nonzero(\pi)$ which returns 1 if none of the elements in π is zero; Otherwise, it returns 0. Temporary power allocations are executed $\frac{M}{2} + \frac{M}{4} + \cdots + 1 = O(M)$ times in each iteration where $\frac{M}{2}$ is the number of groups on Level 1, $\frac{M}{4}$ is the number of groups on Level 2,$\cdots$. Besides, $O(N)$ power levels are tried in each temporary power allocation. In either Step 1" or Step 2", the time complexity is $O(MNT)$.

IV. NUMERICAL RESULTS

In this section, we present the results for both Algorithm 1 and Algorithm 2 and compare them with the combinatorial algorithm. We assume that the power range can be discretized by 1 unit, leading to $N = P_{max}$. The iteration step size h is 10^{-5}. The number of iterations T for all cases is chosen as 10^4. We randomly choose channel gains, and noise levels. Note that the correlations based on geometry is captured in the random cases since channel gain is a function of distance. Noise can be caused by lots of factors such as location, weather, etc. So randomness in noise generation is totally practical.

We start with the three-transmitter case. Channel-related parameters are in Table I and P_{max} is chosen as 10. Moreover, we choose $\beta_1 = 0.8$, $\beta_2 = 0.6$, $\beta_3 = 0.4$, and $\vec{q}(0) = [0.5 \ 0.4 \ 0.3]'$. We generate 100 sets of random numbers for channel-related parameters and plot $|\sum_{i=1}^{3} U_i(\vec{P}) - D(\vec{q^*})|/D(\vec{q^*})$ (no duality gap, so $D(\vec{q^*})$ is the optimal solution to (1)) over these cases in Figure 2. Algorithm 1 deviates from the global optimum by no more than 20% in 90% of the cases. In all cases, the deviation is consistently less than 30%.

We also compared the performance of Algorithm 2 with that of Algorithm 1 in three-transmitter and eight-transmitter cases respectively. Note that the combinatorial algorithm requires

---

Algorithm 2 Greedy Algorithm for Multi-transmitter Case

1: **for all** t in $\{0, \cdots, T-1\}$ **do**
2:    Sort APs by $q_i(t)$ and re-index them from 1 to M
3:    **for all** i in $\{1, \cdots, M\}$ **do**
4:       $\pi^i \leftarrow [0, \cdots, 0, P_{max}, 0, \cdots, 0]$ where P_{max} is the ith element and others are 0
5:    **end for**
6:    **for all** ι in $\{1, \cdots, \lceil \log M \rceil\}$ **do**
7:       **for all** ϱ in $\{1, \cdots, M/2^\iota\}$ **do**
8:          $\psi \leftarrow \pi^\varrho + \pi^{\varrho+1}$
9:          $\omega \leftarrow \vec{q}(t)\vec{r}(\psi)$
10:          **if** $\vec{q}(t)\vec{r}(\pi^\varrho) > \vec{q}(t)\vec{r}(\pi^{\varrho+1})$ **then**
11:             **while** $Nonzero(\pi^{\varrho+1})$ **do**
12:                $\pi^{\varrho+1} \leftarrow \pi^{\varrho+1} - [P_{max}/N]_M$
13:                $\kappa \leftarrow \vec{q}(t)\vec{r}(\pi^\varrho + \pi^{\varrho+1})$
14:                **if** $\kappa > \omega$ **then**
15:                   $\omega \leftarrow \kappa$
16:                   $\psi \leftarrow \pi^\varrho + \pi^{\varrho+1}$
17:                **end if**
18:             **end while**
19:          **else**
20:             **while** $Nonzero(\pi^\varrho)$ **do**
21:                $\pi^\varrho \leftarrow \pi^\varrho - [P_{max}/N]_M$
22:                $\kappa \leftarrow \vec{q}(t)\vec{r}(\pi^\varrho + \pi^{\varrho+1})$
23:                **if** $\kappa > \omega$ **then**
24:                   $\omega \leftarrow \kappa$
25:                   $\psi \leftarrow \pi^\varrho + \pi^{\varrho+1}$
26:                **end if**
27:             **end while**
28:          **end if**
29:          $\pi^\varrho \leftarrow \psi$
30:       **end for**
31:    **end for**
32:    **for all** i in $\{1, \cdots, M\}$ **do**
33:       $q_i(t+1) \leftarrow \{q_i(t) - h[r_i(\pi^1) - \frac{\beta_i}{q_i(t)} + 1]\}^+$
34:    **end for**
35: **end for**
36: $\vec{q}(0) \leftarrow \vec{q}(T+1)$
37: **for all** t in $\{0, \cdots, T-1\}$ **do**
38:    Sort APs by geographical closeness to AP 1 and re-index them from 1 to M
39:   Repeat Lines 3-34
40: **end for**
41: **return** π^1

---

much longer running time than Algorithm 1 (10^8 vs $2^8 \cdot 10^4 + 10^4$). So we only compare the performance of Algorithm 2 with that of Algorithm 1. Although Algorithm 2 performs well with its polynomial complexity in our simulation, it has no benchmark to compare with if we keep increasing the number of transmitters as Algorithm 1 has exponential complexity.

We define *percent effiency of greedy algorithm* as $(U(greedy) - U(Asymp))/U(Asymp)$ where $U(greedy)$ is the maximum value achieved by the objective function of the

TABLE I
PARAMETERS OF THREE-TRANSMITTER CASES

| g_{ij}	j=1	j=2	j=3
i=1	0.9	0.8	0.5
i=2	0.2	0.9	0.4
i=3	0.2	0.3	0.7
	τ_1	τ_2	τ_3
	0.9	0.7	0.3
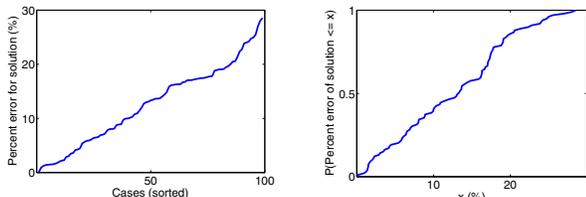
(a) Percent efficiency of solution   (b) Corresponding empirical CDF

Fig. 2. $\sum_{i=1}^{3} U_i(\vec{P})$ and $D(\vec{q^*})$ comparison in 100 three-transmitter cases. Percent efficiency sorted in ascending order.

overall problem with the Algorithm 2 and $U(Asymp)$ is the counterpart with Algorithm 1. The *percent efficiency of greedy algorithm* in three- and eight-transmitter cases are shown in Figures 3(a) and 3(b) separately. In Figure 3(a), Algorithm is not as good as Algorithm 1 in 95% of the cases. In the best case, Algorithm 2 outperforms Algorithm 1 by 3% since the latter is not global optimum. When $\vec{g}, \vec{\tau}$ lead to $\vec{P^*}$ with a large number of P_{max} elements, $\|\vec{d^0}\|$ is large. By Equation (10), Algorithm 1 has a larger gap from the global optimum than in other cases. As a result, Algorithm 2 has a chance to catch up with or even surpass Algorithm 1 in terms of performance. On average, the performance of Algorithm 2 is 20% worse while we reduce the time complexity from exponential to polynomial. Scalability of Algorithm 2 is investigated in Figure 3(b). Parameters we use for eight-transmitter cases are $P_{max} = 20$, $\vec{\beta} = (0.6712, 0.7152, 0.6421, 0.4190, 0.3908, 0.8161, 0.3174, 0.8145)$ and $\vec{q(0)} = (0.5985, 0.6706, 0.7192, 0.8453, 0.9052, 1.1166, 1.1950, 1.4851)$. Similarly, Algorithm 2 loses in the performance comparison in almost all cases. However, Algorithm 2 is on average 14% worse than Algorithm 1, which is better than in three-transmitter cases. Note that when M increases, $\|\vec{d^0}\| = \sqrt{\sum_{i=1}^{M} (d_i^0)^2}$ tends to increase as well. By Equation (10), the efficiency bound of global optimum and Algorithm 1, on average, is bigger in eight-transmitter case than in three-transmitter case. However, Algorithm 2, which is a heuristic, does not suffer from this.

V. CONCLUSION

In this paper, we investigate the power control problem for single-hop AP-based wireless networks under the SINR interference model. We propose an asymptotically optimal algorithm that reduces the time complexity from $O(N^M)$ to $O(N^{M/2})$ in a general case, and to $O(N + T)$ for the special case of $M = 2$. We also identify scenarios in which the time complexity is $O(1)$ when $M = 2$. However, the generalization of this approach to $M > 2$ still remains elusive at this point, which is also one of our future research directions. Inspired
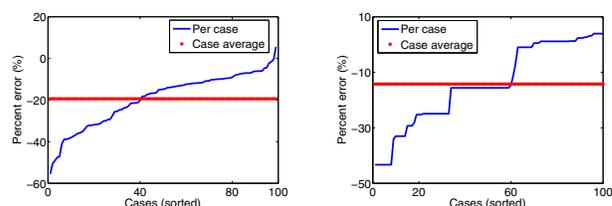
(a) Three-transmitter cases   (b) Eight-transmitter cases

Fig. 3. *Percent efficiency of greedy algorithm* in three- and eight-transmitter cases.

by the structure of the asymptotically optimal algorithm, we also propose a two-stage greedy algorithm with polynomial time complexity. This greedy algorithm has demonstrated performance levels comparable to that of the asymptotically optimal algorithm. In our future work, we will also investigate the performance bound of the greedy algorithm theoretically.

REFERENCES

[1] E. Altman, K. Avrachenkov, I. Menache, G. Miller, B.J. Prabhu, and A. Shwartz. Dynamic discrete power control in cellular networks. *Automatic Control, IEEE Transactions on*, 54(10):2328 –2340, oct. 2009.

[2] Loc X. Bui, Sujay Sanghavi, and R. Srikant. Distributed link scheduling with constant overhead. *IEEE/ACM Trans. Netw.*, 17(5):1467–1480, 2009.

[3] P. Chaporkar, K. Kar, Xiang Luo, and S. Sarkar. Throughput and fairness guarantees through maximal scheduling in wireless networks. *Information Theory, IEEE Transactions on*, 54(2):572 –594, feb. 2008.

[4] Mung Chiang. Balancing transport and physical layers in wireless multihop networks: jointly optimal congestion control and power control. *Selected Areas in Communications, IEEE Journal on*, 23(1):104 – 116, jan. 2005.

[5] Gordon Royle Chris Godsil. *Algebraic Graph Theory*. New York: Springer, 2001.

[6] Shiyang Deng, Tobias Weber, and Andreas Ahrens. Capacity optimizing power allocation in interference channels. *International Journal of Electronics and Communications*, 63(2):139, Feb. 2009.

[7] A. Eryilmaz, O. Asuman, and E. Modiano. Polynomial complexity algorithms for full utilization of multi-hop wireless networks. In *INFOCOM 2007. 26th IEEE International Conference on Computer Communications. IEEE*, pages 499 –507, may 2007.

[8] Libin Jiang and J. Walrand. Stable and utility-maximizing scheduling for stochastic processing networks. In *Communication, Control, and Computing, 2009. Allerton 2009. 47th Annual Allerton Conference on*, pages 1111 –1119, sept. 2009.

[9] Changhee Joo, Xiaojun Lin, and Ness B. Shroff. Understanding the capacity region of the greedy maximal scheduling algorithm in multihop wireless networks. *IEEE/ACM Trans. Netw.*, 17(4):1132–1145, 2009.

[10] Krishnan Kumaran and L. Qian. Uplink scheduling in cdma packet-data systems. In *INFOCOM 2003. Twenty-Second Annual Joint Conference of the IEEE Computer and Communications. IEEE Societies*, volume 1, pages 292 – 300 vol.1, 30 2003.

[11] Shuang Li, Eylem Ekici, and Ness Shroff. Technical report. Power Control for AP-Based Wireless Networks under the SINR Interference Model: Complexity and Efficient Algorithm Development, 2010. http://www.cse.ohio-state.edu/~lish/Shuang_Li_TR_2010.pdf

[12] Xiaojun Lin and N.B. Shroff. The impact of imperfect scheduling on cross-layer congestion control in wireless networks. *Networking, IEEE/ACM Transactions on*, 14(2):302–315, April 2006.

[13] A. Nedic and V.G. Subramanian. Approximately optimal utility maximization. In *Networking and Information Theory, 2009. ITW 2009. IEEE Information Theory Workshop on*, pages 206 –210, 12-10 2009.

[14] N. Z. Shor, Krzysztof C. Kiwiel, and Andrzej Ruszcaynski. *Minimization methods for non-differentiable functions*. Springer-Verlag New York, Inc., New York, NY, USA, 1985.

[15] L. Tassiulas and A. Ephremides. Stability properties of constrained queueing systems and scheduling policies for maximum throughput in multihop radio networks. *Automatic Control, IEEE Transactions on*, 37(12):1936 –1948, dec 1992.